Proceedings of the ASME 2020
International Mechanical Engineering Congress and Exposition
IMECE2020
November 16-19, 2020, Portland, OR, USA

SAND2020-8084C

IMECE2020-23489

MINIMIZING RESIDUAL STRESS IN BRAZED JOINTS BY OPTIMIZING THE BRAZING THERMAL PROFILE

Ben Mann[1]
ATA Engineering, Inc.
San Diego, CA

Kurtis Ford, Mike Neilsen, Dan Kammler
Sandia National Laboratories
Albuquerque, NM

ABSTRACT

Ceramic to metal brazing is a common bonding process used in many advanced systems such as automotive engines, aircraft engines, and electronics. In this study, we use optimization techniques and finite element analysis utilizing viscoplastic and thermo-elastic material models to find an optimum thermal profile for a Kovar® washer bonded to an alumina button that is typical of a tension pull test. Several active braze filler materials are included in this work. Cooling rates, annealing times, aging, and thermal profile shapes are related to specific material behaviors. Viscoplastic material models are used to represent the creep and plasticity behavior in the Kovar® and braze materials while a thermo-elastic material model is used on the alumina.

The Kovar® is particularly interesting because it has a Curie point at 435°C that creates a nonlinearity in its thermal strain and stiffness profiles. This complex behavior incentivizes the optimizer to maximize the stress above the Curie point with a fast cooling rate and then favors slow cooling rates below the Curie point to anneal the material. It is assumed that if failure occurs in these joints, it will occur in the ceramic material. Consequently, the maximum principle stress of the ceramic is minimized in the objective function. Specific details of the stress state are considered and discussed.

Keywords: Brazing, ceramic, optimization

NOMENCLATURE

CTE	Coefficient of thermal expansion, linear
FEM	Finite element model
MPa	$1x10^6$ Pascals

1. INTRODUCTION

Because of the high strength of ceramic and ability to withstand elevated temperatures, it is often used in advanced systems that require bonding with metal parts. Brazing is an ideal technique to join ceramic and metal. Typically, a braze joint is heated to the solidus temperature of the braze filler material and then cooled back to room temperature. In most cases, the materials in a braze joint have mismatched stiffnesses and thermal expansions that lead to residual stress during the thermal cool down. These residual stresses reduce the strength of the joint or lead to a potential catastrophic failure. For this reason, it is ideal to determine an optimal brazing thermal profile to minimize the residual stress in the brazed joint which leads to an effectively stronger joint overall.

Torvund et al [1,2] demonstrated that various properties of the thermal profile such as the braze temperature and cooling rate have a direct effect on the thickness of the reaction layer that develops between the ceramic and active braze filler material which impacts the overall shear strength of the brazed joint. Paiva and Barbosa [3] showed that an optimal brazing temperature and annealing time exist for alumina-titanium brazed joints. Both studies use titanium as the base metal. Liu et al [4] concluded that the brazing cooling rate only has a small effect on the joint strength between alumina and steel.

This study focusses on a specific metal, Kovar®, and how its unique properties impact the stress response of a brazed joint. Kovar® is an alloy developed by Carpenter Technology that has been widely used in ceramic-metal joints [5]. Because Kovar®

[1] Contact author: ben.mann@ata-e.com

has a unique thermal strain profile and temperature dependent stiffness due to its Curie point around 435°C, it is beneficial to better understand how brazing profile properties will impact the residual stress and hence the overall joint strength of Kovar-ceramic brazed joints. This paper gives an overview of the investigation into finding an optimal temperature profile for brazing to minimize the residual stress in the ceramic to Kovar® brazed joint. The material models used will be reviewed, a boundary value problem is explored, and a realistic optimal temperature profile is discussed for each studied braze material.

2. METHODS AND MATERIALS

Finite element analysis is used to predict residual stresses in the ceramic button due to thermal loads and the response to an applied tensile load. Six active braze filler materials are included in this work. Viscoplastic material models are used to represent the creep and plasticity behavior in the Kovar and braze materials while a thermo-elastic material model is used for the Alumina.

2.1 Material Properties

Six different braze filler materials are examined in this paper. The solidus temperature of each material is show in Table 1. The coefficient of thermal expansion (CTE) and Young's modulus of each braze material, along with that of Kovar® and Alumina, are shown in Figure 1 and Figure 2, respectively. Most of the braze materials have a constant CTE, except the CuSil which decreases with temperature to about 400°C. All six braze materials have similar temperature dependent stiffnesses. The Alumina CTE decreases fairly linearly as temperature decreases and its stiffness linearly increases as temperature decreases. The Kovar® CTE drastically decreases from 1000ºC to around 435°C. Below 435°C, the Kovar® CTE increases slightly. This same reversal can be seen when examining the Young's modulus curve for Kovar®. At 435°C, the stiffness trend inverts, and the material becomes softer as temperature decreases. This point of inflection is due to the Curie point of the Kovar®. The Curie point is the temperature at which a ferrous material, such as Kovar®, undergoes a magnetic re-ordering from a paramagnet state above the Curie point to a ferromagnet state below [6].

Table 1: Solidus temperatures of each braze material,

Material	Solidus Temperature (°C)
AgCuZr	961
AuGe	356
CuSil	780
InCuSil15	650
NiCuSil	780
Silver	960

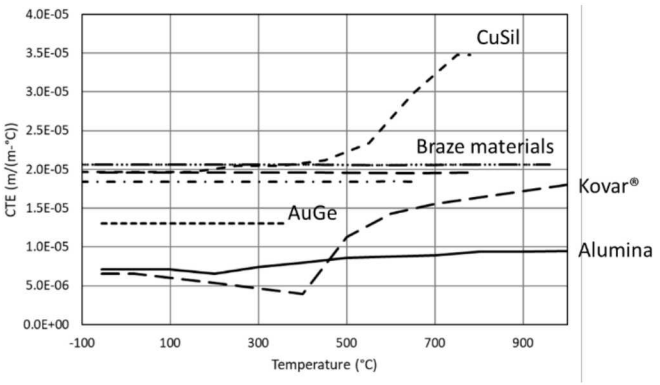

Figure 1: CTE as a function of temperature for all materials used in analysis.

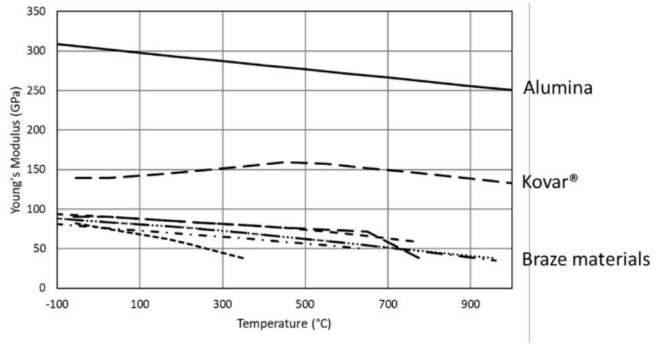

Figure 2: Young's modulus as a function of temperature for all materials used in analysis.

2.2 Material Model Descriptions

The braze materials and the Kovar® alloy are modeled using viscoplastic material models. The viscoplastic material model is a rate- and temperature-dependent model, capturing the creep and plasticity behavior of the material. The material models are correlated with test data at various temperatures and strain rates [7,8]. The Alumina ceramic material is modeled using a simple thermo-elastic material model.

2.3 Finite Element Analysis

A typical button specimen as seen in Figure 3 is composed of two ceramic parts that are brazed to a central washer made of Kovar®. The specimen is modeled using an axisymmetric wedge with half-symmetry assumed about the mid-plane of the washer (Figure 4). A finite element model (FEM) of the geometry is shown in Figure 5. The specimen is heated to the solidus temperature of the braze filler material. At this point, the filler material wets to the ceramic and Kovar® parts. The specimen is then cooled to room temperature and tension is applied to both flanges. The specimen is pulled until fracture.

Sierra SM [9] is used to perform the thermo-mechanical analysis. Two elements through the braze thickness are used to resolve the axial stress in the brazed joint.

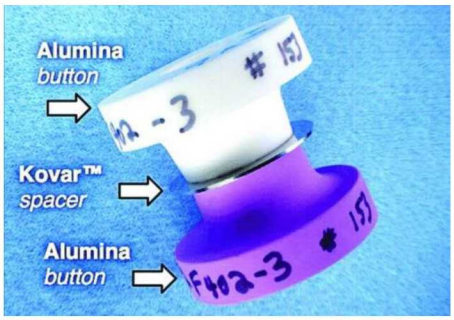

Figure 3: Ceramic button tension test sample [10]

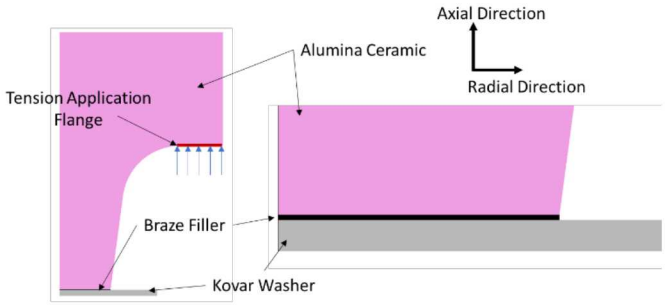

Figure 4: Axisymmetric and half-symmetry FEM of ceramic button with materials and tension application shown. Reference coordinate system is also shown.

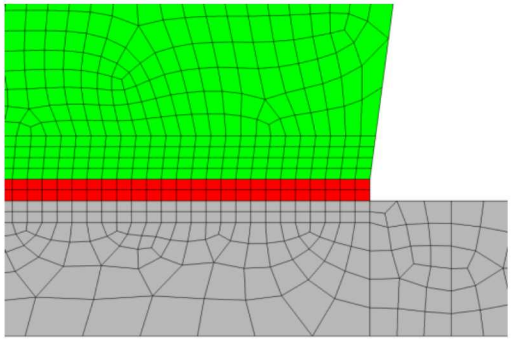
Figure 5: Closeup view of mesh around braze

2.4 Analysis Assumptions

Heat transfer is neglected; the temperature is prescribed uniformly to the entire domain. The specimen is assumed to be free of any cracks or imperfections. When active brazes are used, an interfacial region develops between the braze and adjoining material. This interfacial region is neglected in our analysis.

3. BOUNDARY VALUE PROBLEM

Because of the unique properties of Kovar®, the authors hypothesized that a rapid cooling rate from the solidus temperature to below the Curie point, and a slow cooling rate after, would produce lower residual stresses in the joint. To simulate this hypothesis, several bounding cooling profiles were developed and applied to the ceramic-Kovar® button using AgCuZr as the braze material. These cooling profiles have unrealistic cooling rates but were used to help understand the physics of the problem. Figure 6 shows two of these cooling profiles with zoomed-in portions to demonstrate the change in rate at 300°C. Two additional trivial profiles are run; one has a constant cooling rate of 100°C/sec while the other has a constant cooling rate of 0.01°C/sec.

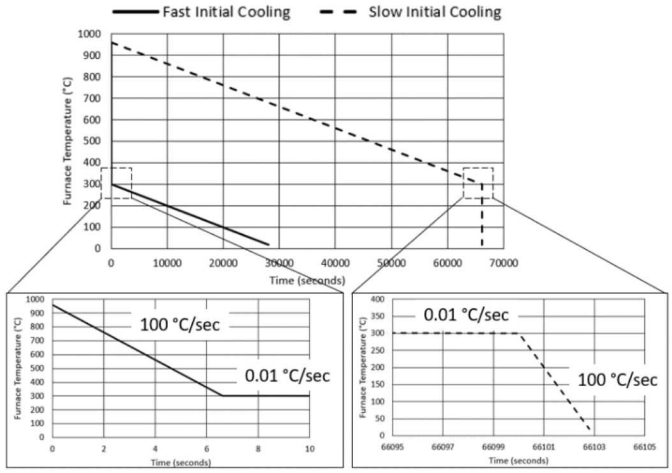

Figure 6: Cooling profiles of bounding cases with details of points where cooling rates change.

Finite element analysis is used to predict residual stresses that develops due to the stiffness and CTE mismatches. These stresses will be analyzed at various points during the cooling profile. The predicted response to a simulated pull test will also be examined.

4. RESULTS OF BOUNDARY VALUE PROBLEM

When analyzing stresses in the ceramic at various temperatures, it becomes evident that a fast initial cooling rate produces higher residual stresses during the cooldown, but lower residual stresses at room temperature. This can be seen when comparing contour plots of stresses for the fast initial cooling rate in Figure 7 with those from the slow initial cooling rate in Figure 8.

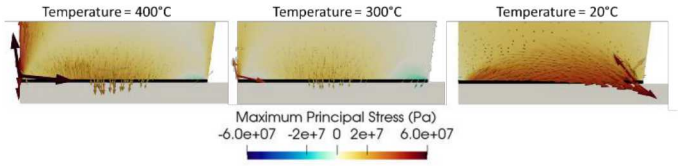

Figure 7: Maximum principal stress at various temperatures for fast initial cooling rate

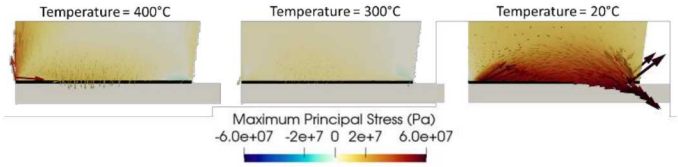

Figure 8: Maximum principal stress at various temperatures during cooling for slow initial cooling rate

This same trend can be seen when looking at the peak maximum principal stress in the ceramic (Figure 9) and the axial stress at the location where the highest stress at room temperature

occurs (Figure 10). The location of peak axial stress at room temperature is shown in Figure 11. The temperature profiles with fast initial cooling rates maximize the peak stress in the ceramic at 400°C. This peak stress is located on the inner diameter of the ceramic button. This is partially due to the large CTE difference between Kovar® and the ceramic up to that point. Notice also from Figure 7 and Figure 8, that compared with the slow initial cooling rate, there is more compression along the outer diameter of the ceramic. This higher amount of compression at 400°C, also seen in Figure 10, leads to a lower magnitude of tension at room temperature.

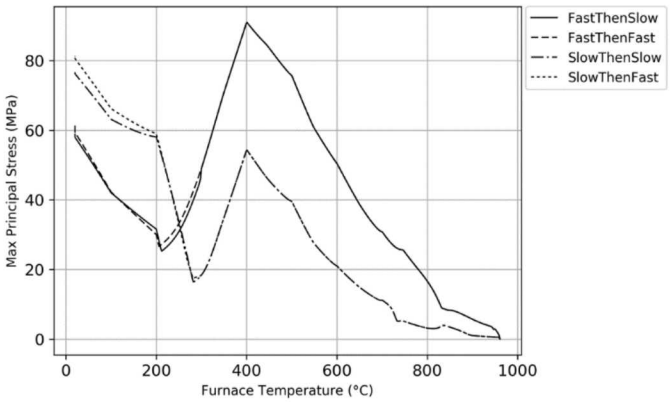

Figure 9: Peak maximum principal stress as a function of temperature for each bounding case

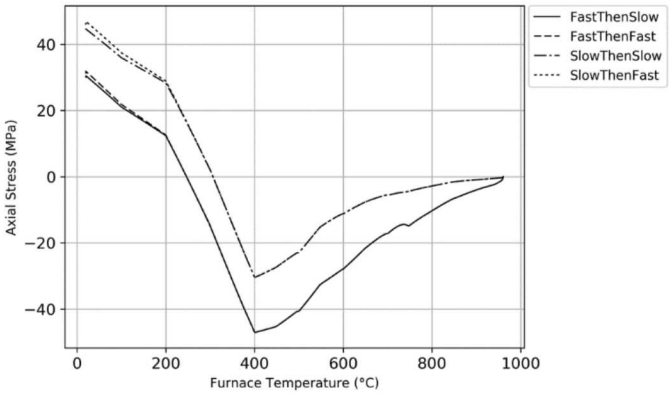

Figure 10: Axial stress for each bounding case at location shown in Figure 11

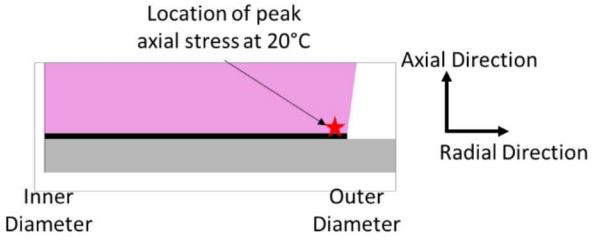

Figure 11: Location of peak axial stress in ceramic at room temperature

The stress state at the ceramic-braze interface is importance because this is typically where failure occurs in the ceramic during tension tests. Axial stress is queried along the interface shown in Figure 12 and is displayed in Figure 13 at 400°C and in Figure 14 at 20°C. The higher amount of compression that builds along the outer diameter at 400°C for the fast initial cooling rate profile leads to a smaller amount of tension in the same location at 20°C. At room temperature, the fast initial cooling rate profile has a maximum axial stress of 30.1 MPa while the slow initial cooling rate profile's maximum axials stress is 46.0 MPa, a difference of 15.9 MPa.

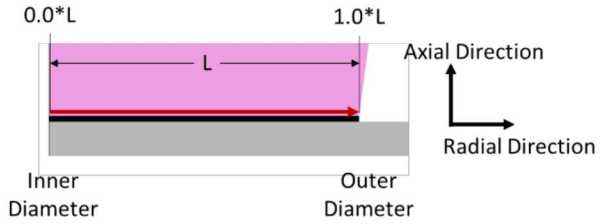

Figure 12: Location of interface plots

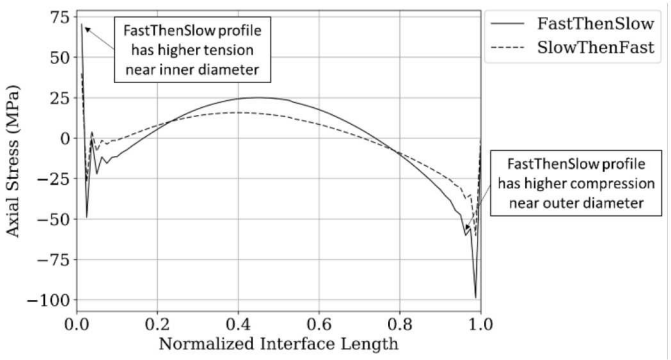

Figure 13: Axial stress in ceramic at braze interface at 400°C for bounding cases

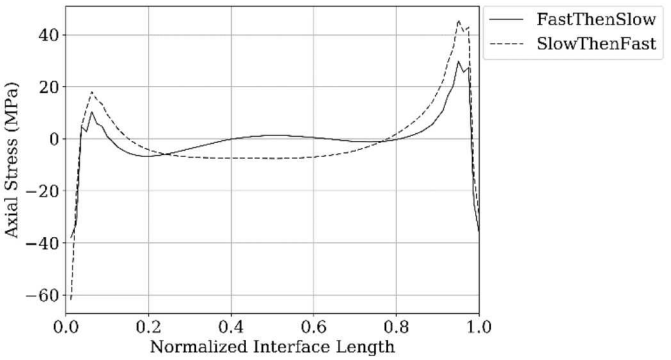

Figure 14: Axial stress in ceramic at braze interface after cooling for bounding cases

After cooling to room temperatures, the simulation continued, and a tensile load was applied to the ceramic button. As seen in Figure 15, at the beginning of the tension pull test, the slow initial cooling profile sample has a larger amount of residual axial stress. This will cause a perceived lower strength, up to a certain point. Because the tensile strength of the ceramic is unknown, and because the ceramic material model does not include any failure criteria, the pull test is simulated to a point

far beyond the expected failure point. The bounding profiles predict that a perceived difference in joint strength can be observed if the absolute tensile strength of the ceramic is less than 150 MPa. For example, if the absolute tensile strength of ceramic was 75 MPa, the fast initial cooling rate sample would fail with an applied load of 5 kN while the slow initial cooling rate sample would fail with an applied load of 3 kN. However, if the actual tensile strength of the ceramic is above 150 MPa, there is no predicted difference in the perceived strength of the joint.

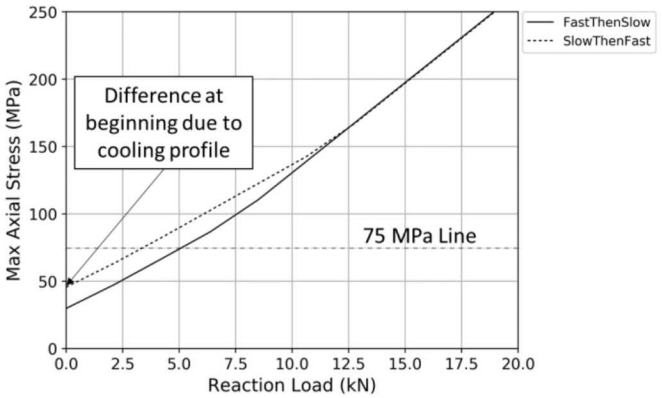

Figure 15: Force-displacement curve from tension test simulation for bounding cases

Before the tensile load is applied, the initial difference in maximum axial stress between the two temperature profiles is due to the residual stress accumulation during cooling. This peak value occurs near the outer diameter of the ceramic button, as seen in Figure 14. As tension is applied to the specimen, the qualitative stress state at the interface remains the same, while the magnitude increases as seen in Figure 16. As more tension is applied, the stress magnitudes in both models continue to increase, but the peak stress location moves away from the interface, and towards the bend point in the ceramic as shown in Figure 17. This implies that if the ceramic tensile strength is greater than 150 MPa, both specimens would fail due to similar loads, but not due to accumulated residual stress from cooling at the braze interface. Instead, the failure would occur near the bend location of the ceramic.

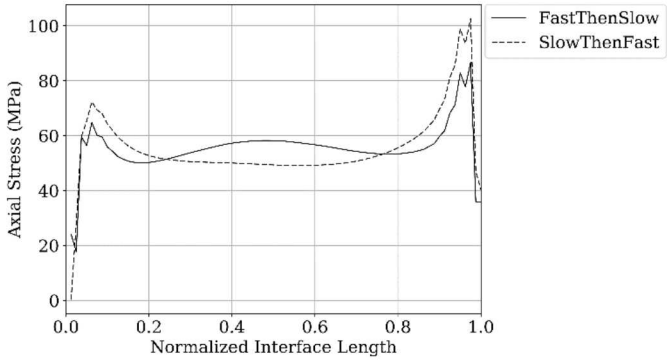

Figure 16: Axial stress in ceramic at braze interface after tension application of 6.4 kN.

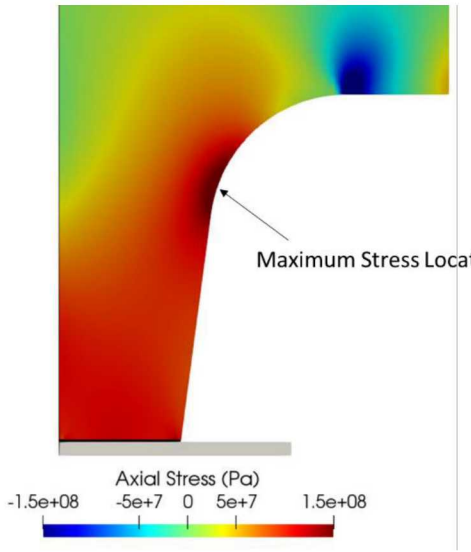

Figure 17: Axial stress contours in ceramic under applied load of 12.5 kN showing maximum stress location in bend area of ceramic.

5. OPTIMIZATION METHODS

After the problem was bounded, an optimization study was performed to discover realistic cooling profiles that minimize residual stresses at room temperature. Along with studying cooling rates, the optimization study incorporated an annealing step to find its impact on the residual stress at room temperature. The ranges of input parameters are shown in Table 2 and a sample cooling profile is shown in Figure 18. The upper anneal temperature is 500°C for all braze materials except AuGe which has an upper limit of 350°C because of its low solidus temperature.

Table 2: Optimization study parameters

Parameter	Range	
	Low	High
Initial Cooling Rate (°C/min)	1	20
Anneal Temperature (°C)	200	Varies
Dwell Time (hours)	0.1	10
Final Cooling Rate (°C/min)	1	20

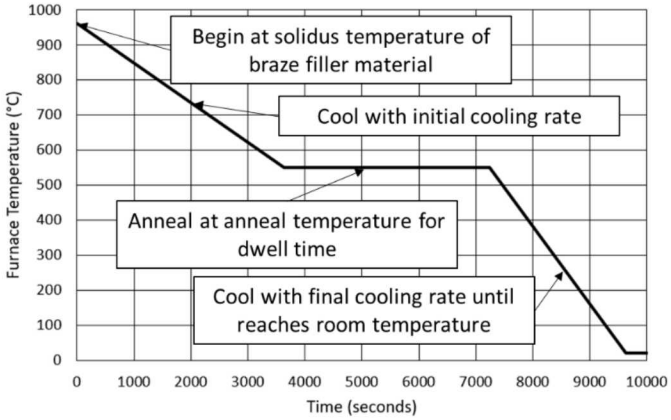

Figure 18: Sample cooling profile for optimization study

The optimization was performed on all six braze filler materials using Dakota, an optimization tool developed by Sandia National Laboratories. An objective function to minimize peak maximum principal stress and peak axial stress in the ceramic at room temperature was developed. An efficient global solver was utilized due to the nonlinearity of the problem space. An additional optimization was performed to attempt to maximize these same variables to predict cooling profiles that lead to high residual stresses. For each braze material, the optimal and least optimal cooling profiles will be shared along with the resulting residual stresses at room temperature.

6. OPTIMIZATION RESULTS

The cooling profile parameters that are found from minimizing the peak stresses at room temperature are shown in Table 3. Table 4 shows the profiles found when the objective function is inverted, finding the profiles with the highest residual stresses at room temperature. As expected, all materials except the AuGe filler drive the optimizer to have fast initial cooling rates. AuGe is different because its solidus temperature is so low, its initial cooling phase is below the Curie point of the Kovar®. All materials also drive the optimizer to have a slow final cooling rate. The anneal temperature is always below the Curie point. Finally, most of the materials drive the optimizer to maximize the dwell time at the anneal temperature; however, this parameter does not have a large effect on the final stress.

Table 3: Cooling profile parameters for minimizing residual stress at room temperature

Material	Initial Cooling Rate (°C/min)	Anneal Temperature (°C)	Dwell Time (hours)	Final Cooling Rate (°C/min)
AgCuZr	20.0	298.2	10.0	1.0
AuGe	1.0	219.9	10.0	5.2
CuSil	18.8	355.5	10.0	1.0
InCuSil15	20.0	200.0	10.0	1.0
NiCuSil	20.0	300.0	7.8	1.0
Silver	20.0	279.2	3.4	1.0

Table 4: Cooling profile parameters for maximizing residual stress at room temperature

Material	Initial Cooling Rate (°C/min)	Anneal Temperature (°C)	Dwell Time (hours)	Final Cooling Rate (°C/min)
AgCuZr	1.0	400.0	10.0	20.0
AuGe	15.8	326.3	0.1	20.0
CuSil	1.0	450.8	10.0	20.0
InCuSil15	7.1	398.0	9.6	17.7
NiCuSil	1.0	455.3	8.9	20.0
Silver	1.0	291.3	4.1	20.0

The residual axial stress at room temperature for the most optimal and least optimal cooling profiles are shown for each material in Table 5.

Table 5: Peak axial stress predictions based on minimizing and maximizing optimization objective function for each braze filler material

Material	Peak Axial Stress (MPa)		
	Minimum	Maximum	Difference
AgCuZr	38.2	45.0	6.8
AuGe	40.8	53.7	12.9
CuSil	43.6	53.0	9.4
InCuSil15	46.8	60.6	13.9
NiCuSil	36.6	47.7	11.0
Silver	12.4	16.0	3.6

To understand the overall impact of each input parameter on the peak axial stress at room temperature, results from each case in the AgCuZr optimization were plotted against the inputs. Figure 19 shows a strong correlation between the initial cooling rate and the peak axial stress at room temperature. Also shown is the impact of the anneal temperature.

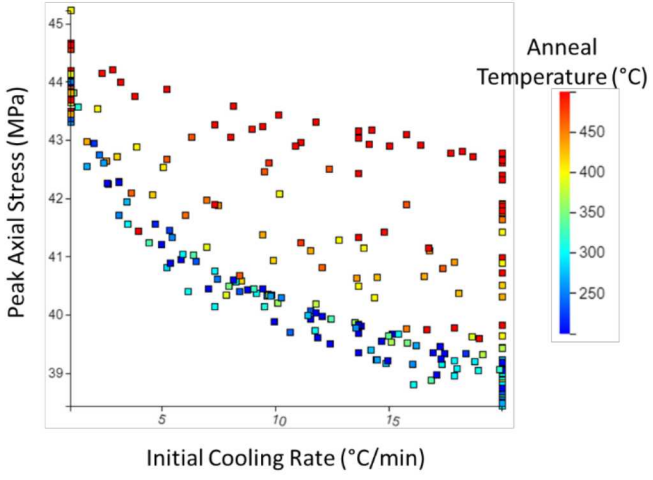

Figure 19: Peak axial stress at room temperature against the initial cooling rate.

Figure 20 shows that there is almost no correlation between the final cooling rate and minimizing the peak axial stress. Finally, Figure 21 demonstrate that the dwell time does not have a large impact on the peak axial stress.

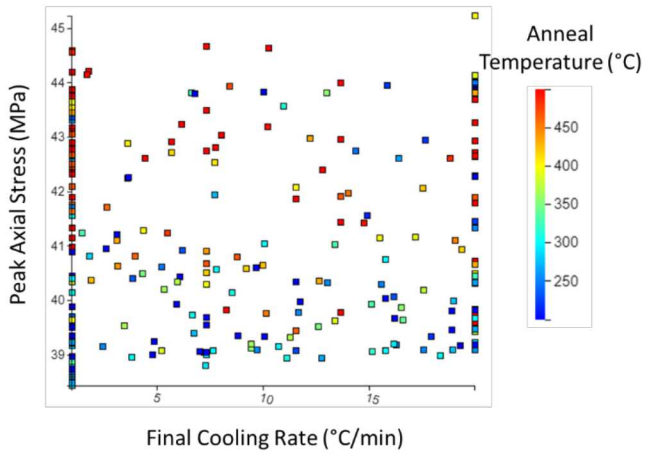

Figure 20: Peak axial stress at room temperature against the final cooling rate.

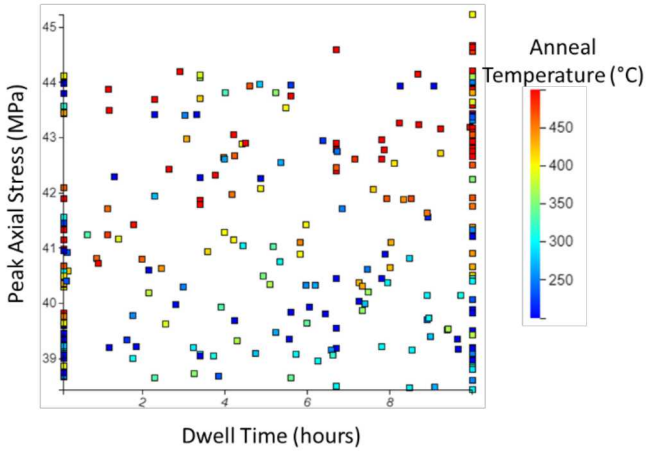

Figure 21: Peak axial stress at room temperature against the dwell time.

7. CONCLUSIONS

Finite element analysis was completed to simulate bounding brazing cooling profiles and predict residual stresses in a Kovar-ceramic brazed joint. Tension loads were simulated to predict failure loads. It was determined that a fast initial cooling rate lead to lower residual stresses from cooling, and a higher perceived joint strength.

An optimization analysis was performed on several braze filler materials to identify other cooling profile parameters that would impact residual stress. A maximum initial cooling rate and an annealing temperature below the Curie point of Kovar® were required to minimize the axial residual stress in the ceramic.

ACKNOWLEDGEMENTS

Sandia National Laboratories is a multi-mission laboratory managed and operated by National Technology and Engineering Solutions of Sandia, LLC., a wholly owned subsidiary of Honeywell International, Inc., for the U.S. Department of Energy's National Nuclear Security Administration under contract DE-NA0003525.

REFERENCES

[1] Torvund, T., Grong, Ø., Akselsen, O.M., and Ulvensøen, J.H. "A process model for active brazing of ceramics." *Journal of Materials Science* Vol. 31 (1996): pp. 6215–6222. DOI 10.1007/BF00354441. https://doi.org/10.1007/BF00354441.

[2] Torvund, T., Grong, Ø., Akselsen, O.M. et al. "A process model for active brazing of ceramics: Part II Optimization of brazing conditions and joint properties." *Journal of Materials Science* Vol. 32 (1997): pp. 4437–4442. DOI 10.1023/A:1018696528510. https://doi.org/10.1023/A:1018696528510.

[3] Paiva, O.C. and Barbosa, M.A. "Brazing parameters determine the degradation and mechanical behaviour of alumina/titanium brazed joints." *Journal of Materials Science* Vol. 35 (2000): pp. 1165–1175. DOI 10.1023/A:1004776117823. https://doi.org/10.1023/A:1004776117823.

[4] Liu, G, Qiao, G., Wang, H., Wang, J., and Lu, T. "Bonding Mechanisms and Shear Properties of Alumina Ceramic/Stainless Steel Brazed Joint." *J. of Materi Eng and Perform* Vol. 20 (2011): pp. 1563–1568. DOI 10.1007/s11665-011-9840-4. https://doi.org/10.1007/s11665-011-9840-4.

[5] "Selecting Controlled Expansion Alloys." *Carpenter Technology*, www.carpentertechnology.com/en/alloy-techzone/technical-information/alloy-selection/selecting-controlled-expansion-alloys.

[6] Hofmann, Philip. *Solid State Physics: An Introduction.* John Wiley & Sons, Berlin (2008).

[7] Stephens, John, Rejent, Jerome, and Schmale, David. "Elevated temperature creep properties of the 54Fe-29Ni-17Co "Kovar" alloy." Technical Report No. SAND2009-0398P, Sandia National Laboratories, Albuquerque, NM. 2009.

[8] Stephens, John and Neilsen, Michael. "Mechanical behavior of the Ag-2Zr and Ag-1Cu-2Zr active braze alloys." *Proceedings of the 3rd International Brazing and Soldering Conference*. pp. 226–233. San Antonio, TX, April 23-26, 2006.

[9] SIERRA Solid Mechanics Team. "Sierra/Solid Mechanics 4.48 User's Guide." Technical Report No. SAND2018-2961, Sandia National Laboratories, Albuquerque, NM. 2018. DOI. 10.2172/1433781. https://doi.org/10.2172/1433781.

[10] Vianco, P., Walker, C., De Smet, D., Kilgo, A., McKenzie, M., and Grant, R. "Interface Reactions Responsible for Run-Out in Active Brazing: Part 1." *Welding Journal* Vol. 97 (2018): pp. 35s-54s. DOI 10.29391/2018.97.004.